Coulomb Stress Changes by Fault Slip and Pore Pressure Push due to Fluid Injection

Ju Hyi Yim[1] , Kwang-Il Kim [1], and Ki-Bok Min[1*]
[1]*Seoul National University, Seoul, Korea*
**kbmin@snu.ac.kr(corresponding author's E-mail)*

Abstract

In hydraulic stimulation, fault slip and pore pressure push are competing mechanisms for stress perturbation which contributes to induced seismicity. Since the fault slip is the irreversible mechanism distinguished from the pore pressure push, considering both mechanisms are difficult numerically and analytically. Interestingly, each mechanism was used independently and gave theoretical insights for various observation related to the seismicity (Segall and Lu, 2015; Steacy et al., 2005). To verify those approaches, the detailed comparison between fault slip and pore pressure push will give the concrete theoretical background. In addition, ignoring the minor mechanism will contribute to the high performance of the numerical simulation and the rigorous simplification for the analytic prediction.

Comsol Multiphysics was used to model the poroelasticity and the fault slip at the same time. To overcome the limitation of continuum-based modeling, the plasticity module was adopted with the Coulomb Failure Criteria as a yield function. The equivalent poisson's ratio and elastic modulus was applied to the fracture zone to model the normal opening of the fracture by the pore pressure.

In this study, fault slip and pore pressure push were compared in two generic cases of the fluid injection into impermeable and permeable matrices. All cases were assumed to contain a single fracture with the aseismic slip. The Coulomb stress changes were calculated on hypothetical fractures parallel to the defined fracture. As a result, the conditions for the dominance of one effect against the other effect were suggested.

Keywords: Coulomb Stress, Enhanced Geothermal System, Shut-in, Induced Seismicity

Introduction

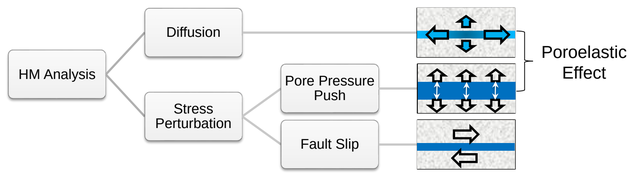

In hydro-mechanical coupling analysis for the fractured medium, driving mechanisms for the induced seismicity are the diffusion and the stress perturbation. According to the diffusion theory, Shapiro (2015) suggested the way to estimate the reservoir diffusivity from the envelope for the seismicity distance and time plot. By using the poroelasticity including the effect of pore pressure push, Segall and Lu (2015) analytically modeled the post-injection seismicity. On the other hand, fault slip induces significant stress perturbation around events so subsequent events can be triggered. The stress perturbation by fault slip could be assessed by calculating Coulomb Failure Stress (CFS) change from the field data. (Steacy et al, 2005; Catalli et al., 2013). This mechanism can be more significant due to the aseismic slip. Guglielmi et al. (2015) observed that substantial portion of aseismic slip among the total slip during the fluid injection, and Louis De Barros et al. (2017) concluded that the stress transfer by the aseismic slip could be the reason for the following induced seismicity.

In this study, the stress perturbation by fault slip was compared with the stress perturbation by pore pressure push in the generic cases. Determination of dominance between fault slip and pore pressure push will give the rigorous background for the current analysis of induced seismicity and help the simplification of the seismicity problems numerically and analytically.

Method

Comsol Multiphysics is Continuum-based finite element method (FEM) code. To model the fracture, I assumed the fracture zone with 1m thickness and applied the plasticity. The Mohr-Coulomb criterion for the fracture slip was applied as the user defined yielding function (Equation 2). By modifying the poisson's ratio and the elastic modulus to make the equivalent model under no lateral displacement condition (Equation 1), the normal opening by the joint normal stiffness was reflected in the fracture zone. Input parameters are based on Chang and Segall (2016) shown in Table 1. Fixed and zero stress boundary were applied because this study focused on the change of CFS, and CFS change was calculated on the left lateral slip of the given fault orientation (60˚ from x axis).

$$v_f' = \frac{1}{1+\left[\frac{v_m}{1-v_m}\frac{\alpha_m}{\alpha_f}+\frac{E_m v_m}{(1+v_m)(1-2v_m)TK_n}\right]}$$

$$E_f' = \frac{E_m v_m}{(1+v_m)(1-2v_m)}\frac{(1+v_f')(1-2v_f')}{v_f'} \quad \dots\dots(1)$$

$$n_f = n_m\left(1-\frac{e_f}{T}\right)+\frac{e_f}{T}$$

v : Poisson's Ratio, α : Biot's Coefficient , E: Young's Modulus,
T: Thickness of Fracture Zone, K_n: Joint Normal Stiffness,
e : Aperture, n : Porosity $'$: Equivalent $_m$: Matrix, $_f$: Fracture Zone

For the fast computation, the plasticity was calculated every interval during short duration. The purpose of this study was the stress perturbation by the poroelasticity and following slip, so the precise time-dependent behavior by fully coupled model was out of the scope.

-Calculating Process

i th step : calculate $\sigma_{n,eff}^{i}$, τ^{i}

i+1 th step : calculate plastic strain by making yielding function (F) as 0

$$F = \frac{\tau^{i+1}}{\mu} - \sigma_{n,eff}^{i} \quad \dots\dots(2)$$

τ : shear stress, $\sigma_{n,eff}$: effective normal stress, μ : friction coefficient

And calculate $\sigma_{n,eff}^{i+1}$, τ^{i+1}

Table 1 . Input Parameters for numerical modeling

	Case 1		Case 2	
	Basement	Fault	Reservoir	Fault
α, Biot's Coefficient	0.2353	1	0.2667	1
E, Young Modulus (MPa)	60000	-	24000	-
ν, Poisson's ratio	0.2	-	0.2	-
n, Porosity	0.05	0.02	0.25	0.02
ρ, Density (kg/m^3)	2740	2500	2500	2500
k, Permeability (m^2)	2.00E-17	6.67E-13	5.00E-15	6.67E-13
K_n, Joint Normal Stiffness (MPa/m)	-	50000	-	50000
L, Fracture Length (m)	-	500	-	500
T, Fracture Thickness (m)	-	1	-	1
e, Fracture Aperture (m)	-	0.0003	-	0.0003
Friction Angle (degree)	-	30	-	30
Cohesion (Mpa)	-	0	-	0
P_{cri}, Critical Pore Pressure (MPa)	-	10	-	0.1
Q, Flow Rate (kg/m/s)	1		0.1	

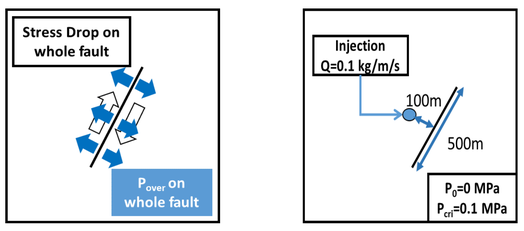

Figure 1. Model Diagram of (Right) Case 1 and (Left) Case 2

Result

- Case 1 : Single fracture model

To determine the dominance of the stress perturbation by fault slip and pore pressure push in actual situation, the seismic data from Basel EGS site was used. The wellhead pressure reached 29.6 MPa and the seismic events reached approximately 500m from the injection point during the injection stage (Figure 2, Right). In contrast, the M_L3.4 earthquake had the source radius of 101m (Häring et al., 2008), which can be linked to approximately stress drop larger than 10 MPa under circular crack model by considering 2.95 moment magnitude measured by Deichmann et al. (2014) (Figure 2, Left). Except for the largest earthquake, the stress drop on average was around 2.3 MPa in Basel (Goertz-Allmann et al., 2011), so the effect of M_w1.5 earthquake can be plotted in the center of Figure 2. According to the Figure 2, the largest magnitude earthquake forms the dominant stress change comparing to the pore pressure push, but the M_w1.5 earthquake effect is minor and less dominant. However, earthquakes over M_w1.5 occurred many times in Basel as time passed, so the cumulative effect may be comparable with the effect of pore pressure push.

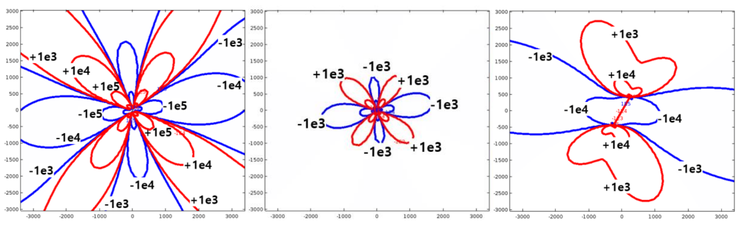

Figure 2. (a) Coulomb stress change distribution by fault slip with (stress drop)=10 MPa, L=200 m and (b) with (stress drop)=2.3 MPa, L=70 m. (c) Coulomb stress change distribution by pore pressure push with (overpressure)=29.6MPa, L=1km. Numbers mean the CFS change.

To assess the total stress perturbation by fault slip, an aseismic slip should be considered in addition to seismic slip. In case of Basel, the sum of moments in seismic event list in Deichmann et al. (2014) was around Mw 3.19 corresponding to the circular rupture with 244m radius and 2.3 MPa stress drop (G = 30 GPa). However, the seismic cloud had almost two times larger radius and the wellhead pressure reached almost 30 MPa. Under the assumption of the single fault and the same average stress drop over this fault, 8 times of moment were expected comparing to the seismic moments. Therefore, the considerable aseismic slip and much larger stress perturbation than Figure 2(a&b) were expected.

- Case 2 : Fluid injection to the permeable matrix containing critically oriented fracture

Chang and Segall (2016) conducted numerical simulation to analyze the poroelastic effect to the seismicity at the reservoir. In Case 2, the poroelastic effect was assessed with the fault slip induced by the fluid injection.

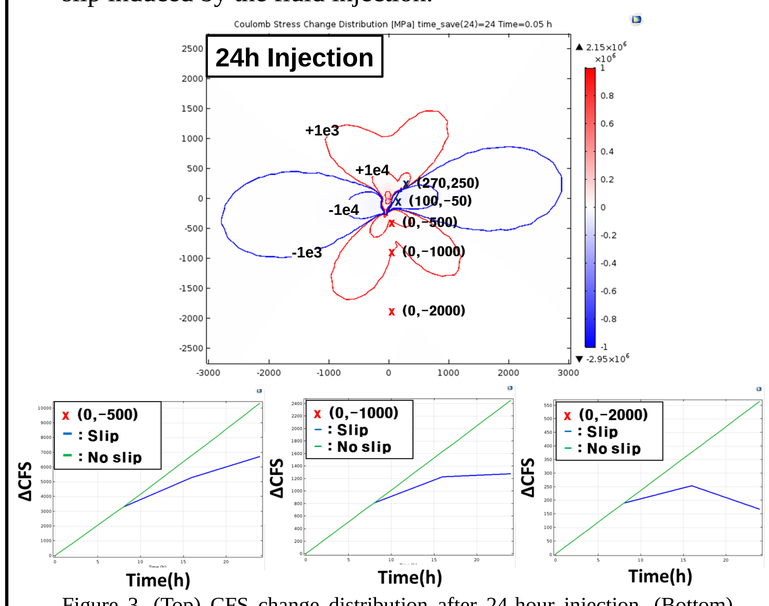

Figure 3. (Top) CFS change distribution after 24-hour injection. (Bottom) CFS change histories at different points below injection point. X marks are the locations of history plots.

The stress perturbation by the fault slip increased gradually as time passed. In the scale of current simulation, the fault slip generally induced less stress perturbation than the poroelastic effect did, but Figure 3 shows that the effect of fault slip is relatively larger in farther area.

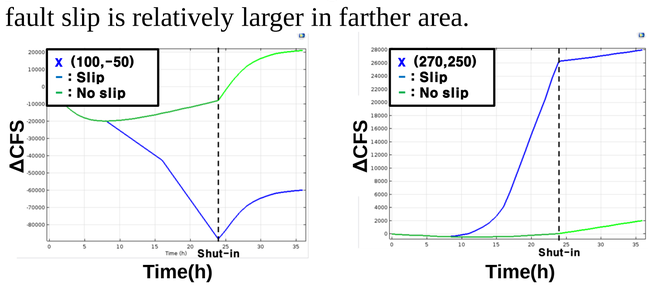

Figure 4. CFS change histories at different points with shut-in.

Figure 4 shows exceptions for the poroelastic analysis by Segall and Lu (2015) due to the dominance of stress perturbation by fault slip near the fault. It was plotted under the assumption of no slip occurring after shut-in.

Conclusions

When the stress perturbation is reflected in physical analysis, the pore pressure push can be ignored comparing to the fault slip by the large magnitude event over 3, but the detailed determination of the dominance has better to be based on the site specific data. The aseismic slip should be considered in addition to the seismic slip if the fault slip should be assessed properly. Even for the permeable reservoir, the critically oriented faults induced the moderate shearing effect.

As a limitation, every numerical analysis was based on 2D simulation, so the stress perturbation can be exaggerated. Due to the singularity around the shearing surface, the numerical instability were unavoidable, but it did not make significant change in the large scale result. Those limitations had better to be fixed for precise modeling, not for this study.

References

Segall, Paul, and S. Lu. "Injection-induced seismicity: Poroelastic and earthquake nucleation effects." Journal of Geophysical Research: Solid Earth 120.7 (2015): 5082-5103.

Steacy, Sandy, Joan Gomberg, and Massimo Cocco. "Introduction to special section: Stress transfer, earthquake triggering, and time-dependent seismic hazard." Journal of Geophysical Research: Solid Earth 110.B5 (2005).

Catalli, Flaminia, Men-Andrin Meier, and Stefan Wiemer. "The role of Coulomb stress changes for injection-induced seismicity: The Basel enhanced geothermal system." Geophysical Research Letters 40.1 (2013): 72-77.

Guglielmi, Yves, et al. "Seismicity triggered by fluid injection–induced aseismic slip." Science 348.6240 (2015): 1224-1226.

De Barros, Louis, et al. "Seismicity and fault aseismic deformation caused by fluid injection in decametric in-situ experiments." Comptes Rendus Geoscience 350.8 (2018): 464-475.

De Simone, Silvia, Jesús Carrera, and Víctor Vilarrasa. "Superposition approach to understand triggering mechanisms of post-injection induced seismicity." Geothermics 70 (2017): 85-97.

Chang, K. W., and P. Segall. "Injection-induced seismicity on basement faults including poroelastic stressing." Journal of Geophysical Research: Solid Earth 121.4 (2016): 2708-2726.

Häring, Markus O., et al. "Characterisation of the Basel 1 enhanced geothermal system." Geothermics 37.5 (2008): 469-495.

Deichmann, Nicholas, Toni Kraft, and Keith F. Evans. "Identification of faults activated during the stimulation of the Basel geothermal project from cluster analysis and focal mechanisms of the larger magnitude events." Geothermics 52 (2014): 84-97.

Goertz-Allmann, Bettina P., Alex Goertz, and Stefan Wiemer. "Stress drop variations of induced earthquakes at the Basel geothermal site." Geophysical Research Letters 38.9 (2011).